

# Homogeneous Conversion of Methane to Methanol. 2. Catalytic Activation of Methane by *cis*- and *trans*-Platin: A Density Functional Study of the Shilov Type Reaction

Kausala Mylvaganam,<sup>†</sup> George B. Bacskay,<sup>†</sup> and Noel S. Hush<sup>\*,†,‡</sup>

Contribution from the School of Chemistry, University of Sydney, NSW 2006, Australia

Received August 19, 1999. Revised Manuscript Received November 29, 1999

**Abstract:** The C–H activation of methane catalyzed by *cis*- and *trans*-platin in aqueous solution has been studied by density functional based computational methods. By analogy with the Shilov reaction, the initial step is the replacement of an ammonia ligand by methane, followed by the formation of a methyl complex and the elimination of a proton. The computations utilize the B3LYP hybrid functionals, effective core potentials, and double- $\zeta$  to polarized double- $\zeta$  basis sets and include solvation effects by a dielectric continuum method. In contrast with the Shilov reaction studied by Siegbahn and Crabtree (*J. Am. Chem. Soc.* **1996**, *118*, 4442), in the platins the replacement of an ammonia ligand by methane is found to be effectively rate determining, in that the energy barriers to C–H activation are comparable with those of the initial substitution reaction, viz.  $\sim 34$  and  $44$  kcal/mol for *cis*- and *trans*-platin, respectively. Several reaction pathways for C–H activation and subsequent proton elimination were identified. For *cis*-platin the energy barriers associated with the oxidative addition and  $\sigma$ -bond metathesis type mechanisms were found to be comparable, while for *trans*-platin oxidative addition is predicted to be strongly preferred over  $\sigma$ -bond metathesis, which, interestingly, also proceeds through a Pt(IV) methyl hydrido complex as reaction intermediate. In line with accepted ideas on trans influence, the methyl and hydride ligands in the Pt(IV) complexes that arise in the oxidative addition reactions were always found to be *cis* to each other. On the basis of the population analyses on the Pt(IV) complexes it is suggested that the Pt–H and Pt–CH<sub>3</sub> bonds are best described as covalent bonds and, further, that the preference of the hydride and methyl anions to be *cis* to each other is a consequence of such covalent bonding. In light of these findings, the energies of several methyl Pt(IV) hydrido bisulfate complexes were also recalculated, with CH<sub>3</sub> and H placed *cis* to each other. The revised results provide evidence for the thermodynamic feasibility of oxidative addition of methane to catalysts such as [Pt(NH<sub>3</sub>)<sub>2</sub>(OSO<sub>3</sub>H)<sub>2</sub>] or [Pt(NH<sub>3</sub>)<sub>2</sub>(OSO<sub>3</sub>H)(H<sub>2</sub>SO<sub>4</sub>)]<sup>+</sup>.

## Introduction

The catalytic conversion of methane to methanol is a problem of considerable scientific and economic importance. Methane, currently our cheapest and most abundant natural hydrocarbon resource, is underutilized by industry because of its high transport and storage costs. Most current technologies convert methane to methanol, which is already a major feedstock in the chemical industry, via the generation of “syngas” (CO + H<sub>2</sub>), whereby methane is fully oxidized at a high temperature. The potential benefits of an economical low-temperature alternative to the syngas technology are obviously great, and as a consequence, much current research is devoted to this problem. As the direct oxidation of methane to methanol involves the activation and functionalization of only one of the C–H bonds of methane, the obvious challenge is to find catalysts that could enable these reactions to proceed at reasonably low temperatures.

The oxidation of methane by platinum salts in solution, i.e., via homogeneous catalysis, was first reported in the 1970s by Shilov and co-workers, and by now there is a considerable body of literature on the subject that report a range of transition metal

compounds that catalyze oxidation.<sup>1–10</sup> The mechanism proposed by Shilov et al.<sup>5,7</sup> for alkane oxidation consists of three basic steps: (a) activation of the alkane by a Pt(II) complex producing an alkyl Pt(II) complex which (b) is oxidized to a Pt(IV) alkyl intermediate that (c) will undergo reductive elimination, yielding the oxidized alkane (alkyl alcohol, ester, halide, etc.) and the original Pt(II) catalyst.

Unfortunately, thus far, commercial developments have been hampered by low yields, slow kinetics, and the poisoning of the catalysts. Recently, Periana et al.<sup>11</sup> reported the successful activation and functionalization of methane in H<sub>2</sub>SO<sub>4</sub>, by bis-(2,2'-bipyrimidine)Pt<sup>II</sup>Cl<sub>2</sub>, that resulted in a 70% one pass yield of methanol. This followed their earlier work that explored the

(2) Davies, J. A.; Watson, P. L.; Liebman, J. L.; Greenberg, A., Eds. *Selective Hydrocarbon Activation*; Wiley-VCH: New York, 1990.

(3) Hill, C. L. *Activation and Functionalization of Alkanes*; Wiley-Interscience: New York, 1989.

(4) Sen, A. *Acc. Chem. Res.* **1988**, *21*, 421.

(5) Shilov, A. E. *Activation of Saturated Hydrocarbons by Transition Metal Complexes*; D. Riedel Publishing Co.: Dordrecht, The Netherlands, 1984.

(6) Waltz, K. M.; Hartwig, J. F. *Science* **1997**, *277*, 211.

(7) Shilov, A. E.; Shul'pin, G. B. *Chem. Rev.* **1997**, *97*, 2879.

(8) Goldberg, K. I.; Wick, D. D. *J. Am. Chem. Soc.* **1997**, *119*, 10235.

(9) Bromberg, S. E.; Yang, H.; Asplund, C. M.; Lian, T.; McNamara, K. B.; Kotz, K. T.; Yeston, J. S.; Wilkens, M.; Frei, H.; Bergman, R. G.; Harris, C. B. *Science* **1997**, *278*, 260.

(10) Hall, C.; Perutz, R. N. *Chem. Rev.* **1996**, *96*, 3125.

(11) Periana, R. A.; Taube, D. J.; Gamble, S.; Taube, H.; Satoh, T.; Fuji, H. *Science* **1998**, *280*, 560.

<sup>†</sup> School of Chemistry, University of Sydney.

<sup>‡</sup> Department of Biochemistry, University of Sydney, NSW 2006, Australia

(1) Arndtsen, B. A.; Bergman, R. G.; Mobley, T. A.; Peterson, T. H. *Acc. Chem. Res.* **1995**, *28*, 154.

feasibility of mercuric salts as catalysts.<sup>12</sup> Inspired by the successful experiments of Periana et al., we recently undertook a quantum chemical study of the thermochemistry of the *cis*-platin-catalyzed process in H<sub>2</sub>SO<sub>4</sub>, in an effort to test the thermodynamic feasibility of several possible reaction pathways using theoretical techniques.<sup>13</sup> We found that the process proposed by Periana et al.,<sup>11</sup> and also by Labinger, Bercaw, and their co-workers,<sup>14,15</sup> where the crucial activation step occurs as an electrophilic attack on CH<sub>4</sub> by a solvated [Pt(NH<sub>3</sub>)<sub>2</sub>-(OSO<sub>3</sub>H)]<sup>+</sup> molecule (T-complex), is thermodynamically feasible. The activation reaction is followed by oxidation of the resulting methyl complex to a bisulfate ester. While the homogeneous catalytic process of Periana et al.<sup>11</sup> represents an obvious breakthrough, it would be obviously desirable if such a catalysis could be carried out in solvents that are more benign than concentrated H<sub>2</sub>SO<sub>4</sub>. Very recently Johansson et al. observed C–H activation under mild conditions in 2,2,2-trifluoroethanol (TFE) at a cationic Pt(II) diimine aqua complex,<sup>16</sup> which represents an obvious advance in this area.

Our previous study was restricted to a study of the thermodynamics of the key reactions of the methane → methyl bisulfate ester conversion in sulfuric acid, and as such, it did not include the elucidation of full details of the reaction pathways, such as transition states and possible further intermediates. Given the large sizes of the mono- and bis(bisulfate) intermediates that are present in the reaction schemes considered, a detailed exploration of the potential energy surface represents a considerably more complex and resource-intensive study but one which we hope to complete soon.

In an effort to gain useful insight and understanding of the factors that affect every step of the C–H activation process, we thought it instructive to carry out in the first instance a series of detailed studies on a simpler system: [PtCl<sub>2</sub>(NH<sub>3</sub>)<sub>2</sub>]. Siegbahn and Crabtree<sup>17</sup> have recently made a theoretical study of the Shilov reaction involving [PtCl<sub>2</sub>(H<sub>2</sub>O)<sub>2</sub>], where in the initial reaction step a water ligand is found to be replaced by a CH<sub>4</sub> molecule in the first coordination shell. In our studies of the analogous reaction schemes for the related [PtCl<sub>2</sub>(NH<sub>3</sub>)<sub>2</sub>] (*cis* and *trans*) an ammonia ligand is initially replaced by CH<sub>4</sub>. As the metal–ammonia bond in these complexes is expected to be considerably stronger than the metal–water bond in the aqua complexes, the activation energy for the transfer of CH<sub>4</sub> into the first coordination shell is likely to be proportionately higher for the *cis*- and *trans*-platin reactions—in fact, this ligand exchange may not be the most energetically favorable reaction pathway. (As shown by the experiments of Periana et al.,<sup>11</sup> as well as our previous theoretical work,<sup>13</sup> *cis*-platin readily activates methane in sulfuric acid, where the first step is loss of chloride.) However, our interest is generally in an analysis of the effects of the nature of ligation on the reaction pathways and energetics, and in this work we are concerned with the theoretical comparison of H<sub>2</sub>O and NH<sub>3</sub> replacement.

A fundamental question is whether the reaction of CH<sub>4</sub> with a metal complex leading to C–H bond breaking and formation of a metal–CH<sub>3</sub> bond proceeds by electrophilic substitution ( $\sigma$ -

bond metathesis) or oxidative addition, involving Pt(II) → Pt(IV) oxidation. For reaction of the *trans*-aqua complex in aqueous acid solution Siegbahn and Crabtree concluded that the most favored pathway was  $\sigma$ -bond metathesis, in which a proton is transferred from a methane  $\sigma$ -complex to a neighboring chloride ligand.<sup>17</sup> This is in effect the mechanism suggested by Shilov.<sup>5,7</sup> However, an oxidative addition pathway was found to be closely competitive and no firm distinction between these could be made on theoretical grounds. We find more complex behavior for the hypothetical *cis*- and *trans*-platin activation of methane by NH<sub>3</sub> replacement, with some marked differences from those noted for the aqua systems. Interestingly, in their recent theoretical study of inter- and intramolecular C–H activation by a cationic iridium(III) complex, Niu and Hall found that the activation process occurs only by oxidative addition, via the formation of a Ir(IV) hydrido complex.<sup>18</sup>

In the course of this mechanistic study we also found that the products of an oxidative addition of CH<sub>4</sub> to a Pt(II) complex would yield Pt(IV) methyl hydrido complexes with the methyl and hydride ligands effectively occupying *cis* positions relative to each other. Moreover, the comparative energetic studies that we also carried out have shown that placing these ligands *trans* to each other yields an energy that is ~35 kcal mol<sup>-1</sup> higher than for the corresponding *cis* isomer. Qualitatively, such an ordering in energy may be predicted on the basis of the strongly *trans*-directing natures of the hydride and methyl ligands,<sup>19,20</sup> but the computed energy difference actually turned out to be larger than expected. Consequently, in light of this observation we have also recalculated the thermodynamics of the oxidative addition of methane to several potential Pt(II) catalysts considered in our previous work, placing CH<sub>3</sub><sup>-</sup> and H<sup>-</sup> ligands *cis* to each other rather than *trans* as had been done before.

## Computational Methods

As in our previous work, the calculations reported in this paper were performed using density functional theory (DFT), utilizing the hybrid functional B3LYP.<sup>21–24</sup> The bulk of the calculations, in particular all geometry optimizations and vibrational frequency calculations, were carried out using the effective core potentials (ecp) and double- $\zeta$  basis sets of Stoll et al.<sup>25,26</sup> for the heavy atoms and a double- $\zeta$  basis set for the H atoms.<sup>27</sup> The resulting (valence) basis is thus a [6s5p3d] set on Pt, accommodating the 16 valence electrons, [2s2p] on C and N, and [2s3p] on Cl and [2s] on H, denoted ecp-DZ. The energies were then recalculated with a larger basis set, which is a full double- $\zeta$  plus polarization set<sup>28,29</sup> on the C, N, Cl and H atoms (with all their electrons) but containing the same Pt ecp and basis as the smaller set described above. This larger basis is denoted ecp-DZP.

The partition functions and hence thermal and zero point corrections to the molecular energies as well as molecular entropies were obtained using the standard formulas for quantum harmonic oscillators and classical rotors as well as classical translation, using the vibrational frequencies and rotational constants computed with the ecp-DZ basis. The solvation free energies were calculated using the isodensity polarized continuum model (IPCM),<sup>30</sup> which is a dielectric continuum

(18) Niu, S.; Hall, M. B. *J. Am. Chem. Soc.* **1998**, *120*, 6169.

(19) Hartley, F. R. *Chem. Soc. Rev.* **1973**, *2*, 163.

(20) Lin, Z.; Hall, M. B. *Inorg. Chem.* **1991**, *30*, 646.

(21) Becke, A. D. *Phys. Rev. A* **1988**, *38*, 3098.

(22) Lee, C.; Yang, W.; Parr, R. G. *Phys. Rev. B* **1988**, *37*, 785.

(23) Vosko, S. H.; Wilk, L.; Nusair, M. *Can. J. Phys.* **1980**, *58*, 1200.

(24) Becke, A. D. *J. Chem. Phys.* **1993**, *98*, 5648.

(25) Igel-Mann, G.; Stoll, H.; Preuss, H. *Mol. Phys.* **1988**, *65*, 1321.

(26) Andrae, D.; Häussermann, U.; Dolg, M.; Stoll, H.; Preuss, H. *Theor. Chem. Acta* **1990**, *77*, 123.

(27) Huzinaga, S. *J. Chem. Phys.* **1965**, *42*, 1293.

(28) Dunning, T. H.; Hay, P. J. In *Modern Theoretical Chemistry*; Schaefer, H. F., III, Ed.; Plenum: New York, 1976; Vol. 3, p 1.

(29) Frisch, M. J.; Pople, J. A.; Binkley, J. S. *J. Chem. Phys.* **1984**, *80*, 3265.

(12) Periana, R. A.; Taube, D. J.; Evitt, E. R.; Löffler, D. G.; Wentreck, P. R.; Voss, G.; Masuda, T. *Science* **1993**, *259*, 340.

(13) Mylvaganam, K.; Bacskey, G. B.; Hush, N. S. *J. Am. Chem. Soc.* **1999**, *121*, 4633.

(14) Luinstra, G. A.; Wang, L.; Stahl, S. S.; Labinger, J. A.; Bercaw, J. E. *J. Organomet. Chem.* **1995**, *504*, 75.

(15) Stahl, S. S.; Labinger, J. A.; Bercaw, J. E. *Angew. Chem., Int. Ed. Engl.* **1998**, *37*, 2180.

(16) Johansson, L.; Ryan, O. B.; Tilset, M. *J. Am. Chem. Soc.* **1999**, *121*, 1974.

(17) Siegbahn, P. E. M.; Crabtree, R. H. *J. Am. Chem. Soc.* **1996**, *118*, 4442.

type method, where the shape and size of the cavity occupied by the solute molecule is defined by an isodensity surface of the solute. Application of the IPCM method has, however, necessitated all electron calculations; these were performed using the ecp-DZ basis at the appropriate (gas phase) optimized geometries, the core orbitals of each atom expanded in terms of Huzinaga's minimal basis sets.<sup>31</sup>

The charge distributions of the complexes were analyzed by the Roby–Davidson<sup>32–35</sup> and the Mulliken methods.<sup>36</sup> In the Roby–Davidson approach the one-electron density is analyzed by defining and using a set of projection operators associated with each atom, as well as all pairs, triples, ..., of atoms, which enables the corresponding calculation of the number of electrons associated with individual atoms and pairs, triples, ..., of atoms. Generally, the most important quantities are the shared electron number between two atoms, which can be correlated with the degree of covalent bonding between those atoms and the net charges on the atoms. In the Mulliken method, the measure of electron sharing is provided by the overlap population.

The methods and basis sets discussed above were used with a good degree of success in our previous work on platinum catalysts as well as molecular hydrogen complexes of osmium(II).<sup>37,38</sup>

The computations were carried out using the Gaussian94 and -98 programs<sup>39,40</sup> using the DEC alpha workstations of the Theoretical Chemistry group at Sydney University.

## Results and Discussion

The reactions considered in this work are the replacement of an ammonia ligand by methane



followed by activation of the CH bond either by  $\sigma$ -bond metathesis yielding  $\text{PtCl}(\text{HCl})(\text{CH}_3)(\text{NH}_3)$  or, oxidatively, by the formation of a Pt(IV) alkyl hydrido complex, viz.  $\text{PtCl}_2(\text{H})(\text{CH}_3)(\text{NH}_3)$ . The final steps are reductive eliminations, where a proton is transferred to the ammonia ligand, so that  $\text{NH}_4^+$  could be eliminated, and hence yielding the Pt(II) complex  $\text{PtCl}_2(\text{NH}_3)(\text{CH}_3)$ . In a study of an analogous set of reactions, namely those of the diaqua complex  $\text{PtCl}_2(\text{H}_2\text{O})_2$ , Siegbahn and

(30) Foresman, J. B.; Keith, T. A.; Wiberg, K. B.; Snoonian, J.; Frisch, M. J. *J. Phys. Chem.* **1996**, *100*, 16069.

(31) Huzinaga, S.; Andzelm, J.; Kobukowski, M.; Radzio-Andelmann, E.; Sakai, Y.; Tatewaki, H. *Gaussian Basis Sets for Molecular Calculations*; Elsevier: Amsterdam, 1984.

(32) Davidson, E. R. *J. Chem. Phys.* **1967**, *46*, 3320.

(33) Roby, K. R. *Mol. Phys.* **1974**, *27*, 81.

(34) Heinzmann, R.; Ahlrichs, R. *Theor. Chim. Acta* **1976**, *42*, 33.

(35) Ehrhardt, C.; Ahlrichs, R. *Theor. Chim. Acta* **1985**, *68*, 231.

(36) Mulliken, R. S. *J. Chem. Phys.* **1955**, *23*, 1833.

(37) Bytheway, I.; Bacskay, G. B.; Hush, N. S. *J. Phys. Chem.* **1996**, *100*, 6023.

(38) Bytheway, I.; Bacskay, G. B.; Hush, N. S. *J. Phys. Chem.* **1996**, *100*, 14899.

(39) Frisch, M. J.; Trucks, G. W.; Schlegel, H. B.; Gill, P. M. W.; Johnson, B. G.; Robb, M. A.; Cheeseman, J. R.; Keith, T.; Petersson, G. A.; Montgomery, J. A.; Raghavachari, K.; Al-Laham, M. A.; Zakrzewski, V. G.; Ortiz, J. V.; Foresman, J. B.; Cioslowski, J.; Stefanov, B. B.; Nanayakkara, A.; Challacombe, M.; Peng, C. Y.; Ayala, P. Y.; Chen, W.; Wong, M. W.; Andres, J. L.; Replogle, E. S.; Gomperts, R.; Martin, R. L.; Fox, D. J.; Binkley, J. S.; Defrees, D. J.; Baker, J.; Stewart, J. P.; Head-Gordon, M.; Gonzalez, C.; Pople, J. A. *Gaussian 94 (Revision E.2)*; Gaussian, Inc.: Pittsburgh, PA, 1995.

(40) Frisch, M. J.; Trucks, G. W.; Schlegel, H. B.; Scuseria, G. E.; Robb, M. A.; Cheeseman, J. R.; Zakrzewski, V. G.; Montgomery, J. A.; Stratmann, R. E.; Burant, J. C.; Dapprich, S.; Millam, J. A.; Daniels, A. D.; Kudin, K. A.; Strain, M. C.; Farkas, O.; Tomasi, J.; Barone, V.; Cossi, M.; Cammi, R.; Mennucci, B.; Pomelli, C.; Adamo, C.; Clifford, S.; Ochterski, J.; Petersson, G. A.; Ayala, P. Y.; Cui, Q.; Morokuma, K.; Malick, D. K.; Rabuck, A. D.; Raghavachari, K.; Foresman, J. B.; Cioslowski, J.; Ortiz, J. V.; Stefanov, B. B.; Liu, G.; Liashenko, A.; Piskorz, P.; Komaromi, I.; Gomperts, R.; Martin, R. L.; Fox, D. J.; Keith, T.; Al-Laham, M. A.; Peng, C. Y.; Nanayakkara, A.; Gonzalez, C.; Challacombe, M.; Gill, P. M. W.; Johnson, B. G.; Chen, W.; Wong, M. W.; Andres, J. L.; Head-Gordon, M.; Replogle, E. S.; Pople, J. A. *Gaussian 98 (Revision A.3)*; Gaussian, Inc.: Pittsburgh, PA, 1998.

Crabtree<sup>17</sup> found that, after methane exchanged with water, the presence of a solvating water molecule, bridging in effect the remaining water ligand and a chloride, has an important energetic effect. We have observed a similar effect in that the  $\text{PtCl}_2(\text{CH}_4)(\text{NH}_3)$  complex could form a fairly strong bond with an ammonia or water molecule by way of a hydrogen bond to the metal-bound ammonia ligand. Therefore we decided to retain both ammonia molecules in our calculations, so the ammonia–methane exchange reaction is rewritten in the form



The ligands inside the brackets are understood to be in the first coordination shell, with the second ammonia being effectively in the second coordination shell but hydrogen bonded to the ammonia ligand. We recognize of course that in an aqueous solution the second ammonia could be replaced by water, so we may well have  $[\text{PtCl}_2(\text{CH}_4)(\text{NH}_3)] \cdots \text{OH}_2$ . It is worth noting that ammonia, when bonded to a metal ion such as  $\text{Pt}^{2+}$ , is quite acidic, i.e., it is a good proton donor, unlike free ammonia which is a very poor proton donor, as evidenced by the very weak H-bond in the ammonia dimer.<sup>41</sup> Very strong hydrogen bonds of this type have been noted before, especially for systems with fluoride as a ligand. In a number of complexes it has been found that fluoride has the capacity to form intramolecular H– bonds with other ligands, such as  $\text{NH}_2$ ,<sup>42</sup> or intermolecular H-bonds with other species, especially HF, in which case the system is best described as a complex of bifluoride.<sup>43,44</sup>

The computed (relative) electronic energies of the molecular species studied in this work that correspond to equilibrium and transition state geometries on the potential energy surfaces and all isomers of *cis*- and *trans*- $[\text{PtCl}_2(\text{NH}_3)_2]\text{CH}_4$  (as well as others studied in this work) along with their solvation energies, zero point energies, entropies, thermal corrections to the enthalpies, and the resulting relative enthalpies and free energies in aqueous solution at 298 K are given in Table 1. The total electronic energies (in  $E_h$ ) are given in Table S1 of the Supporting Information. The structures that correspond to these species, viz. **1C**–**13C** and **1T**–**16T**, will be given in later sections of the paper that discuss the reaction pathways. The corresponding energetic information for the parent *cis*- and *trans*-platin complexes and free ligands is summarized in Table 2 and Table S1. Comparison of the relative ecp-DZ and ecp-DZP energies in Table 1 indicates that there is a reasonably good level of agreement between them, the differences being generally ~3–5 kcal/mol, i.e., ~10–20%, the ecp-DZP relative energies being consistently lower. The largest differences occur for the highest energy transition states and intermediate **6T-TS**, **7T**, and **8T-TS**. Since all the species in the reactions are neutral molecules, the solvation energies are fairly small (~–10 kcal/mol), and thus, the solvent contributions to the reaction energies and barriers are quite modest. Exceptions are the transition state **6C-TS** and **8C-TS** and the formation of the ion pair **13C**.

In the following sections we discuss the results obtained for the reactions between methane and *cis*- and *trans*-platin, respectively, as well as the relative stabilities of  $[\text{PtCl}_2(\text{NH}_3)_2]$  and  $[\text{PtCl}_2(\text{H}_2\text{O})_2]$  and also the stabilities of the Pt(IV) isomers  $[\text{PtCl}_2\text{H}(\text{CH}_3)(\text{NH}_3)_2]$  and  $[\text{Pt}(\text{NH}_3)_2\text{H}(\text{CH}_3)(\text{OSO}_3\text{H})_2]$  and  $[\text{Pt}(\text{NH}_3)_2\text{H}(\text{CH}_3)(\text{OSO}_3\text{H})(\text{H}_2\text{SO}_4)]$ .

(41) Hassett, D. M.; Marsden, C. J.; Smith, B. J. *Chem. Phys. Lett.* **1991**, *183*, 449.

(42) Patel, B. P.; Crabtree, R. H. *J. Am. Chem. Soc.* **1996**, *118*, 13105.

(43) Murphy, V. J.; Hascall, T.; Chen, J. Y.; Parkin, G. *J. Am. Chem. Soc.* **1996**, *118*, 7428.

(44) Whittlesey, M. K.; Perutz, R. N.; Greener, B.; Moore, M. H. *Chem. Commun.* **1997**, 187.



**Table 1.** Platinum Complexes: Relative Gas-Phase Energies, Total and Relative Solvation Energies, Zero-Point Vibrational Energies, Thermal Contributions to Enthalpies, Standard Entropies, and Relative Enthalpies, and Gibbs Free Energies of the *cis*- and *trans*-Platin Based Intermediates and Products Obtained by the Ecp-DZ and Ecp-DZP Basis Sets (in Parentheses) at 298 K<sup>a,b</sup>

| molecule             | $\Delta E^{el}(g)/$<br>kcal mol <sup>-1</sup> | $E_{solv}/$<br>kcal mol <sup>-1</sup> | $E_{ZPE}/$<br>kcal mol <sup>-1</sup> | $H^{therm}/$<br>kcal mol <sup>-1</sup> | $S^{\circ}/$<br>cal K <sup>-1</sup> mol <sup>-1</sup> | $\Delta E^{el}(sol^n)/$<br>kcal mol <sup>-1</sup> | $\Delta H_{298}^{\circ}(sol^n)/$<br>kcal mol <sup>-1</sup> | $\Delta G_{298}^{\circ}(sol^n)/$<br>kcal mol <sup>-1</sup> |
|----------------------|---|---------------------------------------|--------------------------------------|--|---|---|--|--|
| <i>cis</i> -Platin   |   |                                       |                                      |  |   |   |  |  |
| 1C                   | 0   | -7.6                                  | 79.3                                 | 88.4                                   | 125.2   | 0   | 0  | 0  |
| 2C-TS                | 37.0 (34.0)                                   | -7.1                                  | 77.2                                 | 86.2                                   | 118.6   | 37.5 (34.5)                                       | 33.3   | 37.2 (34.2)  |
| 3C                   | 35.6 (30.8)                                   | -7.9                                  | 77.4                                 | 86.4                                   | 118.6   | 35.3 (30.5)                                       | 33.3   | 35.3 (30.5)  |
| 4C-TS                | 35.9 (31.2)                                   | -10.8                                 | 77.3                                 | 86.0                                   | 115.7   | 32.7 (28.0)                                       | 30.3   | 33.1 (28.4)  |
| 5C                   | 26.8 (24.6)                                   | -11.6                                 | 77.9                                 | 86.6                                   | 115.9   | 22.8 (20.6)                                       | 21.0   | 23.8 (21.6)  |
| 6C-TS                | 49.8 (44.8)                                   | -18.1                                 | 74.7                                 | 82.9                                   | 112.3   | 39.3 (34.3)                                       | 33.8   | 37.6 (32.6)  |
| 7C                   | 36.4 (30.8)                                   | -6.9                                  | 75.7                                 | 84.1                                   | 115.4   | 37.1 (31.5)                                       | 32.8   | 35.8 (30.2)  |
| 8C-TS                | 35.1 (32.5)                                   | -15.0                                 | 76.7                                 | 84.7                                   | 110.5   | 27.7 (25.1)                                       | 24.0   | 28.4 (25.8)  |
| 9C                   | 29.3 (29.0)                                   | -12.2                                 | 77.7                                 | 86.0                                   | 115.6   | 24.7 (24.4)                                       | 22.3   | 25.1 (24.8)  |
| 10C-TS               | 31.9 (31.9)                                   | -11.6                                 | 77.7                                 | 85.5                                   | 107.8   | 27.9 (27.9)                                       | 25.0   | 30.1 (30.1)  |
| 11C                  | 14.8 (17.2)                                   | -10.8                                 | 79.3                                 | 87.0                                   | 105.3   | 11.6 (14.0)                                       | 10.2   | 16.1 (18.5)  |
| 12C-TS               | 38.7 (36.9)                                   | -9.5                                  | 76.7                                 | 85.1                                   | 117.3   | 36.8 (35.0)                                       | 33.5   | 35.9 (34.1)  |
| 13C                  | 7.5 (8.5)                                     | -27.1                                 | 79.8                                 | 87.9                                   | 111.3   | -12.0 (-11.0)                                     | -12.5  | -8.4 (-7.4)  |
| <i>trans</i> -Platin |   |                                       |                                      |  |   |   |  |  |
| 1T                   | 0   | -10.3                                 | 79.6                                 | 88.9                                   | 126.9   | 0   | 0  | 0  |
| 2T-TS                | 45.5 (42.8)                                   | -8.6                                  | 77.3                                 | 86.3                                   | 120.2   | 47.2 (44.5)                                       | 44.6   | 46.6 (43.9)  |
| 3T                   | 43.2 (37.9)                                   | -9.9                                  | 77.8                                 | 86.9                                   | 118.6   | 44.9 (38.3)                                       | 42.9   | 45.3 (38.7)  |
| 4T-TS                | 45.0 (39.8)                                   | -10.8                                 | 77.1                                 | 86.1                                   | 118.4   | 45.4 (39.3)                                       | 42.6   | 45.1 (39.0)  |
| 5T                   | 31.0 (28.6)                                   | -10.0                                 | 78.2                                 | 86.9                                   | 117.0   | 31.3 (28.9)                                       | 29.3   | 32.2 (29.8)  |
| 6T-TS                | 72.2 (61.5)                                   | -8.6                                  | 74.3                                 | 82.8                                   | 115.0   | 73.9 (63.2)                                       | 67.8   | 71.3 (60.6)  |
| 7T                   | 70.5 (58.7)                                   | -7.6                                  | 75.4                                 | 84.3                                   | 120.0   | 73.2 (61.4)                                       | 68.6   | 70.7 (58.9)  |
| 8T-TS                | 73.0 (60.6)                                   | -10.2                                 | 75.1                                 | 83.8                                   | 115.4   | 73.1 (60.7)                                       | 68.0   | 71.3 (58.9)  |
| 9T-TS                | 43.5 (40.3)                                   | -10.5                                 | 76.6                                 | 84.8                                   | 112.9   | 43.3 (40.1)                                       | 39.2   | 43.3 (40.1)  |
| 10T                  | 42.3 (39.2)                                   | -8.7                                  | 76.8                                 | 85.3                                   | 114.6   | 43.9 (40.8)                                       | 40.3   | 44.0 (40.9)  |
| 11T-TS               | 43.7 (40.4)                                   | -8.7                                  | 76.8                                 | 84.9                                   | 111.3   | 45.3 (42.0)                                       | 41.3   | 46.0 (42.7)  |
| 12T                  | 25.7 (25.9)                                   | -12.1                                 | 78.8                                 | 87.0                                   | 112.0   | 23.9 (24.1)                                       | 22.0   | 26.4 (26.6)  |
| 13T-TS               | 48.1 (44.7)                                   | -9.1                                  | 77.4                                 | 85.7                                   | 112.1   | 49.3 (45.9)                                       | 46.1   | 50.5 (47.1)  |
| 14T                  | 32.8 (32.2)                                   | -11.7                                 | 77.7                                 | 86.2                                   | 113.5   | 31.4 (30.8)                                       | 28.7   | 32.6 (32.1)  |
| 15T-TS               | 62.0 (58.5)                                   | -9.0                                  | 75.5                                 | 83.9                                   | 113.9   | 63.3 (59.8)                                       | 58.3   | 62.1 (58.6)  |
| 16T                  | 38.9 (36.6)                                   | -10.3                                 | 77.6                                 | 86.1                                   | 116.4   | 38.9 (36.6)                                       | 36.1   | 39.2 (36.9)  |

<sup>a</sup> The systems 1C–13C and 1T–16T represent reactants, products, intermediates, and transition states in the methane activation pathways. All are isomers of *cis*- and *trans*-[PtCl<sub>2</sub>(NH<sub>3</sub>)<sub>2</sub>]CH<sub>4</sub>. <sup>b</sup> Total enthalpies and Gibbs free energies (including solvation) are obtained as  $H_{298}^{\circ}(sol^n) = E^{el} + E_{solv} + H_{298}^{therm}(g)$ ;  $G_{298}^{\circ}(sol^n) = E^{el} + E_{solv} + G_{298}^{therm}(g)$ .  $H_{298}^{therm}(g)$  and  $G_{298}^{therm}(g)$  include the zero-point energy ( $E_{ZPE}$ ) and  $E^{el}$  include nuclear repulsion.

**Table 2.** *cis*- and *trans*-Platin and Ligands: Solvation Energies, Zero-Point Vibrational Energies, and Thermal Contributions to Enthalpies and Standard Entropies at 298 K

| ligands              | $E_{solv}/$<br>kcal mol <sup>-1</sup> | $E_{ZPE}/$<br>kcal mol <sup>-1</sup> | $H^{therm}/$<br>kcal mol <sup>-1</sup> | $S^{\circ}/$<br>cal K <sup>-1</sup> mol <sup>-1</sup> |
|----------------------|---------------------------------------|--------------------------------------|--|---|
| <i>cis</i> -platin   | -9.4                                  | 50.5                                 | 56.7                                   | 95.4  |
| <i>trans</i> -platin | -12.9                                 | 50.7                                 | 56.6                                   | 96.7  |
| Cl <sup>-</sup>      | -63.2                                 |                                      |  |   |
| NH <sub>3</sub>      | -3.6                                  | 20.7                                 | 23.2                                   | 48.5  |
| CH <sub>4</sub>      | -0.1                                  | 28.0                                 | 30.4                                   | 46.7  |
| H <sub>2</sub> O     | -7.1                                  | 12.3                                 | 14.7                                   | 45.2  |

**Relative Stabilities of *cis*- and *trans*-Platin.** According to our computations, *trans*-platin is more stable than its *cis* isomer, in both gas phase and aqueous solution, by ~14 and ~18 kcal/mol, respectively. This is in qualitative agreement with the available experimental data on the relative heats of formation of *cis*- and *trans*-platin in their respective standard (crystalline) states, according to which *trans*-platin is more stable by 3 kcal/mol.<sup>45</sup> There appears to be no such data on the relative stabilities of these isomers in aqueous solution.

Given that *trans*-platin is nondipolar, in contrast with a computed dipole of 12.3 D for *cis*-platin, it may seem somewhat surprising that the *trans* isomer appears to be more highly solvated. The situation is analogous to that noted for the *cis* and *trans* isomers of [PdCl<sub>2</sub>(H<sub>2</sub>O)<sub>2</sub>], where Siegbahn and Crabtree<sup>46</sup> found in their self-consistent reaction field (SCRFF)

calculations that the larger solvation energy of the *trans* isomer is due mostly to the large difference in the quadrupole moments, with nonnegligible octupole and hexadecapole contributions. In our work, use of the IPCM-polarized continuum method effectively bypasses the potential convergence problem of the multipole expansion method but it neglects the nonelectrostatic contributions to the solvation such as dispersion, repulsion, and cavitation.<sup>47</sup>

In a further study of the solvation of *cis*- and *trans*-platin we carried out calculations on these molecules in the presence of four discrete water molecules, optimizing the gas-phase geometries of the resulting [PtCl<sub>2</sub>(NH<sub>3</sub>)<sub>2</sub>](H<sub>2</sub>O)<sub>4</sub> clusters at the B3LYP/epc-DZ level of theory, which was followed by the computation of the solvation energy of each cluster by the IPCM method. The structures obtained are shown in Figure 1. We expected the water molecules to bridge the ammonia and chloride ligands via hydrogen bonds, but such a structure was only obtained for *trans*-platin (structure **A**). In the case of *cis*-platin the optimizations consistently yielded a structure with just one water bridging the two ammonias as well as forming a H-bonded chain with the remaining three water molecules, as shown also in Figure 1. Evidently, the water–water hydrogen bonds are considerably stronger than the alternative water–chloride bonds, etc. Indeed, an alternative *trans*-platin based isomer (structure **B**) was subsequently found, where a given

(46) Siegbahn, P. E. M.; Crabtree, R. H. *Mol. Phys.* **1996**, *89*, 279.

(47) Bacskay, G. B.; Reimers, J. R. In *Encyclopedia of Computational Chemistry*; Schleyer, P. v. R., Ed.; J. Wiley & Sons Ltd.: Chichester, U.K., 1998; p 2620.

(45) Chernyaev, I. I.; Palkin, V. A.; Baranova, R. A.; Kuz'mina, N. N. *Russian J. Inorg. Chem.* **1960**, *5*, 693.

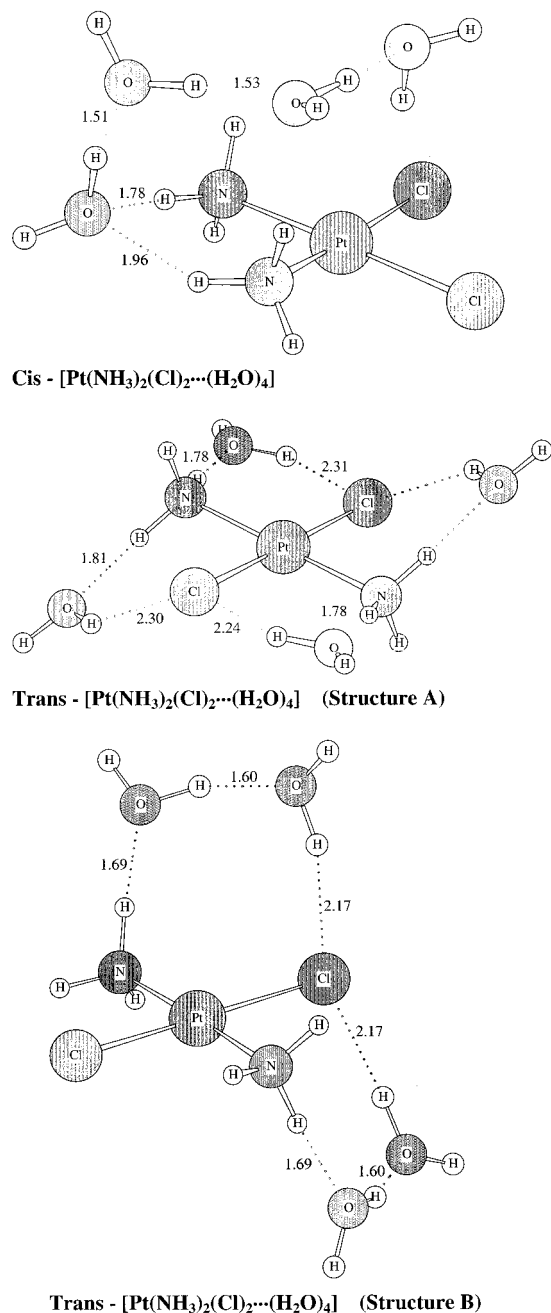
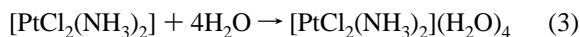


**Figure 1.** Structures of *cis*- and *trans*-[PtCl<sub>2</sub>(NH<sub>3</sub>)<sub>2</sub>](H<sub>2</sub>O)<sub>4</sub> clusters.

pair of ammonia and chloride ligands are bridged by a water dimer, and which has a lower energy. The gas-phase binding energies of the four solvating water molecules, defined as the energies of the reactions



were computed (at the ecp/DZP level, without zero point corrections) as  $-54.9$ ,  $-41.5$ , and  $-45.9$  kcal/mol for the *cis*, *trans* (A), and *trans* (B) isomers, respectively. These results suggest that the *cis* isomer may be better solvated, by up to 9 kcal/mol, as a result of the stronger hydrogen bonds in the former. However, when the secondary solvation effects with the bulk solvent are also calculated, using the IPCM method, the reverse trend is obtained. The computed solvation energies of the three clusters are  $-10.5$ ,  $-16.5$ , and  $-14.2$  kcal/mol. When these results are combined with those from the gas-phase cluster calculations, the difference in overall solvation energies

**Table 3.** Gas-Phase Binding Energies (in kcal/mol) of Ligands in Various Pt(II) Complexes Obtained at the B3LYP/ecp-DZ Level of Theory (without Zero-Point Vibrational Corrections)

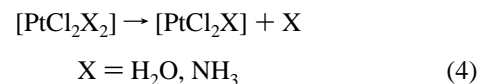
| complex   | ligands         |                 |                  |                   |
|---|-----------------|-----------------|------------------|-------------------|
|   | NH <sub>3</sub> | Cl <sup>-</sup> | H <sub>2</sub> O | CH <sub>4</sub>   |
| <i>cis</i> -PtCl <sub>2</sub> (NH <sub>3</sub> ) <sub>2</sub>   | 51.5            | 151.0           |                  | 7.3 <sup>a</sup>  |
| <i>trans</i> -PtCl <sub>2</sub> (NH <sub>3</sub> ) <sub>2</sub> | 64.4            | 154.4           |                  | 14.5 <sup>a</sup> |
| <i>cis</i> -PtCl <sub>2</sub> (H <sub>2</sub> O) <sub>2</sub>   |                 | 166.6           | 32.1             | 8.6 <sup>b</sup>  |
| <i>trans</i> -PtCl <sub>2</sub> (H <sub>2</sub> O) <sub>2</sub> |                 | 158.6           | 46.4             | 21.6 <sup>b</sup> |

<sup>a</sup> Binding energy of methane in *cis*- and *trans*-PtCl<sub>2</sub>NH<sub>3</sub>CH<sub>4</sub>.

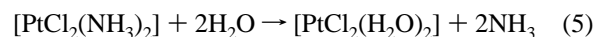
<sup>b</sup> Binding energy of methane in *cis*- and *trans*-PtCl<sub>2</sub>H<sub>2</sub>OCH<sub>4</sub>.

between *cis*- and *trans*-platin is reduced to  $\sim 5$  kcal/mol, in favor of the *cis* isomer. These results, although qualitatively different from the initial IPCM estimates of 3.5 kcal/mol in favor of *trans*-platin (see Table 1), would not significantly alter our earlier conclusion that the *trans* isomer is expected to be more stable in solution. Clearly, however, a significantly larger number of discrete water molecules are needed to adequately model the solvation of these simple platinum complexes. While we cannot rule out the possibility that a more accurate treatment of solvation would yield qualitatively different results, we believe that it is unlikely that the change would be large enough to result in a substantial change in the total *cis*–*trans* energy difference, most of which is electronic in origin.

**Relative Stabilities of the Pt(II) Diammine and Diaqua Complexes.** The Shilov reaction occurs for platinum salts in aqueous acid solution, where the active metal complexes are believed to be diaqua Pt complexes such as [PtCl<sub>2</sub>(H<sub>2</sub>O)<sub>2</sub>]. If the rate-determining step in the alkyl activation reactions is the exchange of methane with an inner-sphere ligand such as water or ammonia, the rate of the overall reaction could be, to a large extent, determined by the endothermicity of that exchange reaction, which will strongly depend on the binding energy of H<sub>2</sub>O or NH<sub>3</sub> in the appropriate complex. These were obtained by computing the (gas phase) energies of the dissociation reactions



The results are given in Table 3, along with the binding energies of CH<sub>4</sub> (in [PtCl<sub>2</sub>(CH<sub>4</sub>)X]) and Cl<sup>-</sup>, which had also been calculated in an analogous fashion. Clearly, ammonia is more tightly bound than water, the difference in their binding energies being  $\sim 19$  kcal/mol. Therefore, the activation energies for the methane–ammonia exchange are expected to be roughly that much higher than for the analogous methane–water exchange. Interestingly, the binding energy of methane depends to a significant degree on the other ligands in the complex. Thus in *trans*-[PtCl<sub>2</sub>(CH<sub>4</sub>)(H<sub>2</sub>O)] methane is computed to be bound by 21.6 kcal/mol, to be compared with 7.3 kcal/mol in *cis*-[PtCl<sub>2</sub>(CH<sub>4</sub>)(NH<sub>3</sub>)]. Therefore the low barrier to methane–water exchange in *trans*-[PtCl<sub>2</sub>(H<sub>2</sub>O)<sub>2</sub>] is probably partly due to the correspondingly low endothermicity of that reaction. Alternatively, considering the energetics of the substitution reaction



we computed (gas phase) reaction energies of 43.7 and 52.7 kcal/mol for the *cis* and *trans* isomers, respectively. These results, in good agreement with the estimates discussed above, indicate that ammonia is bound by  $\sim 24$  kcal/mol more tightly than water.

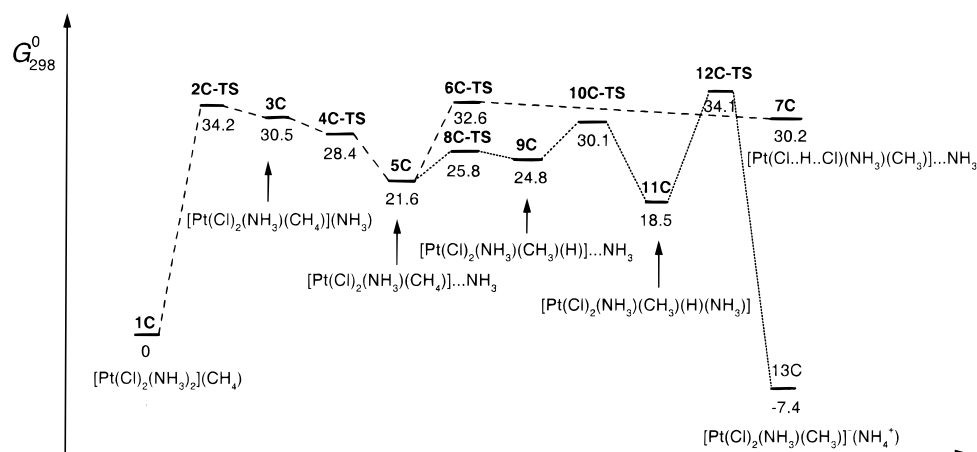


**Figure 2.** Schematic potential energy surface for methane activation by *cis*-platin.

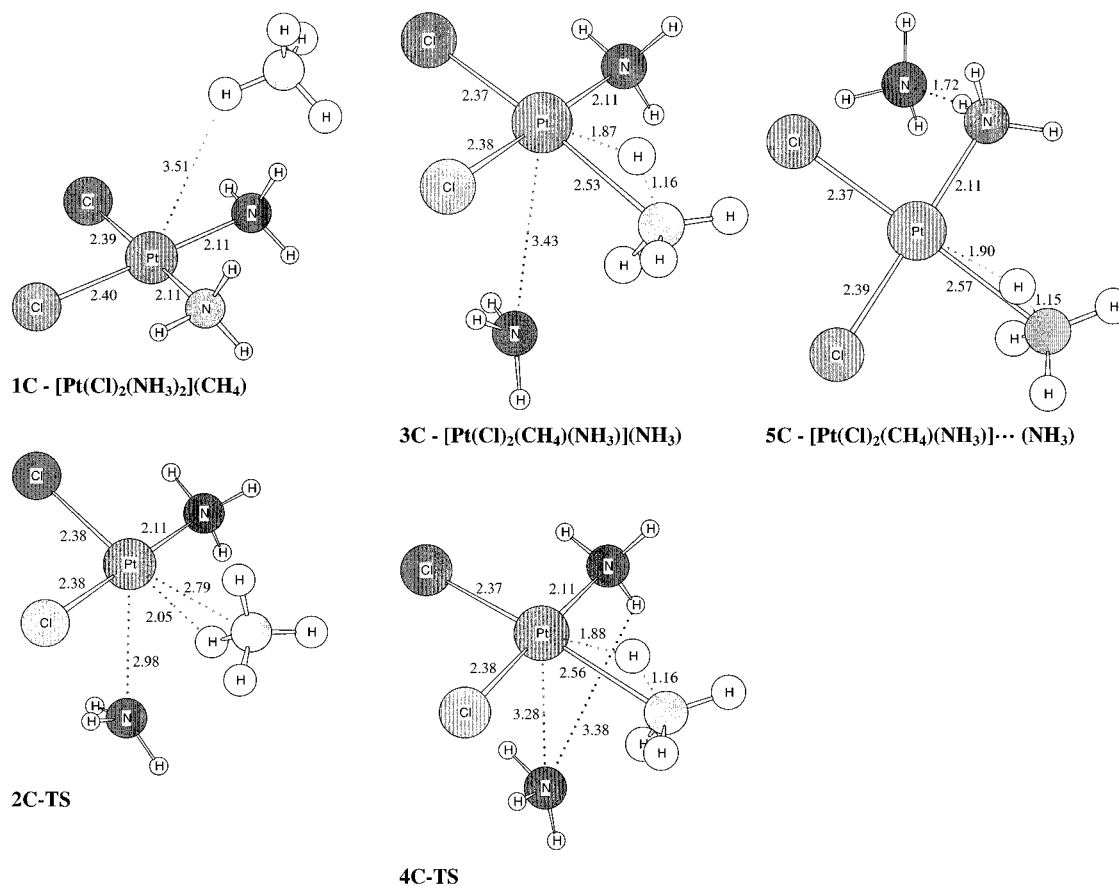
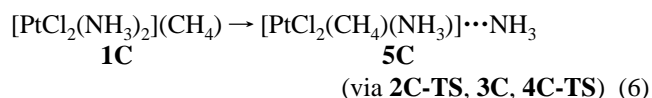


**Figure 3.**  $\text{CH}_4/\text{NH}_3$  exchange in *cis*-platin: Structures of intermediates and transition states.

**Methane Activation by *cis*-Platin.** Two distinct reaction pathways were found in the study of the PES of this reaction, as shown by the diagram in Figure 2. The initial reactant molecule is *cis*-platin (**1C**) with a methane molecule in the second coordination shell. The first reaction is the exchange of this methane with ammonia, producing a complex (**3C**) where methane is now in the inner coordination shell as ligand, while the ammonia, having moved to the second coordination shell, is only weakly bound. The structures associated with this first step are shown in Figure 3. As may be expected, migration of this ammonia molecule so as to hydrogen bond to the ammonia ligand is a facile process, with a very small or no barrier at all. While a small barrier corresponding to **4C-TS** was located at the DFT/ecp-DZ level of theory, as the results in the tables indicate, once solvation and entropic effects are included, the

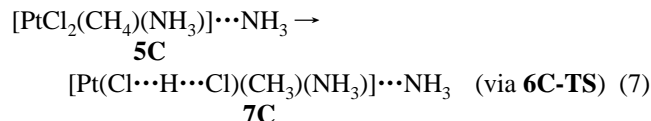
energy barrier located on the gas-phase PES disappears altogether. The net reaction for this first phase is then



where the highest free energy barrier, computed as 34.2 kcal/mol, corresponds to the transition state **2C-TS** for the initial methane–ammonia exchange. By contrast, the barrier for the exchange of methane with water for *cis*-[PtCl<sub>2</sub>(H<sub>2</sub>O)<sub>2</sub>] has been estimated as just 12.8 kcal/mol.

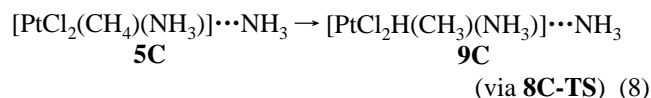
CH activation now can occur in two distinct ways. In the  $\sigma$ -bond metathesis proton migration occurs to the chloride *cis* to methane (see structures in Figure 4) but in such a way that

the proton ends up on the far side of the chloride, so that it bridges the two chlorides, i.e., giving rise to a bichloride:

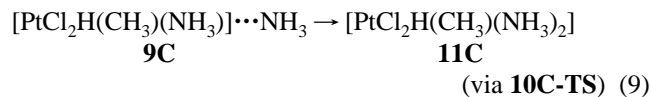


In contrast with the observed bifluoride complexes,<sup>42–44</sup> the bichloride ion in **7C** acts as a bidentate ligand. In the transition state the distance between the migrating hydrogen and the methyl carbon is  $\sim 3.4$  Å, suggesting that the CH bond must be completely broken. Moreover the hydrogen–platinum distance is only 1.85 Å. It was confirmed however that the normal coordinate corresponding to the imaginary frequency ( $454i \text{ cm}^{-1}$ ) effectively describes a large amplitude oscillation of the hydrogen between the carbon and chlorine atoms. Once the product **7C** is formed, it could be deprotonated by a solvent molecule, or by the H-bonded ammonia, resulting in the formation of  $[\text{PtCl}_2\text{H}(\text{CH}_3)(\text{NH}_3)]^-$  and  $\text{NH}_4^+$  or the ion pair **13C**. An alternative, possibly more obvious pathway, where the migrating hydrogen would end up between the methyl and the chloride cis to it, so that it would be bonded to the latter, was also considered. However, as the resulting product was found to lie  $\sim 13$  kcal/mol above **7C**, we did not attempt to locate the transition state associated with this process.

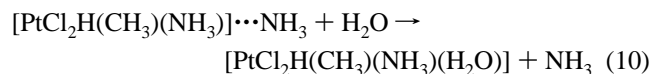
The alternative pathway to  $\sigma$ -bond metathesis is the oxidative addition of methane to *cis*-platin (see structures **8C-TS**–**13C** in Figure 5). In the first step hydrogen migrates to the platinum ion, effectively oxidizing it to Pt(IV):



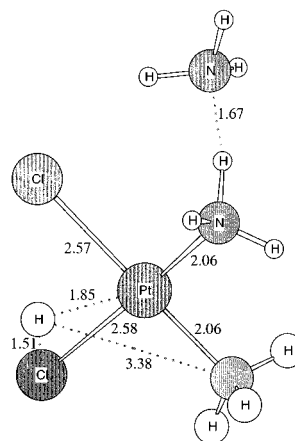
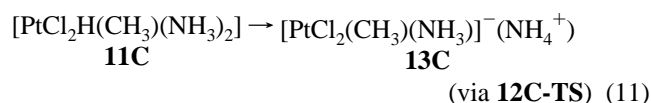
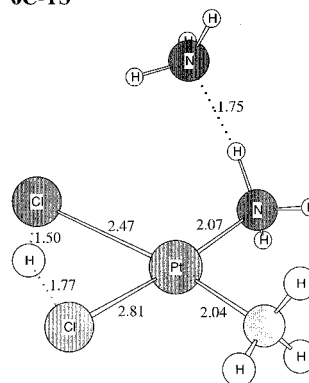
The intermediate **9C** is now a pentacoordinate Pt(IV) complex, best described as a trigonal bipyramid, with the ammonia dimer and a chloride occupying the axial positions. It could become hexacoordinate by a solvating water molecule becoming a ligand or by utilizing the nearby ammonia in the second coordination shell. We considered both possibilities. The latter corresponds to the reaction



which results in an (approximately) octahedral Pt(IV) complex (**11C**) with the methyl and ammonia ligands occupying the axial positions with the hydride being cis to the equatorial ammonia. The alternative, where a water molecule exchanges with an ammonia and moves into the first coordination shell, i.e.



was found to be 9.2 kcal/mol less favorable than reaction 8. Given **11C**, the final step is a highly concerted reaction that enables Pt(IV) to revert to Pt(II), while the platinum–axial ammonia bond is broken as the hydrogen, as proton, migrates to the leaving ammonia

**6C-TS****7C** -  $[\text{Pt}(\text{Cl} \cdots \text{H} \cdots \text{Cl})(\text{CH}_3)(\text{NH}_3)] \cdots (\text{NH}_3)$ 

**Figure 4.** C–H activation by  $\sigma$ -bond metathesis in *cis*-platin: Structures of intermediates and transition states.

resulting in a highly stable ion pair (**13C**), where an ammonium ion is hydrogen bonded to the two chloride ligands. A hypothetical alternative to this process is the concerted, one-step isomerization of **9C** to **13C**, corresponding to a simultaneous migration of the hydrogen and ammonia to the chlorines. However, the barrier for this reaction was found to be  $\sim 33$  kcal/mol (relative to **9C**), which effectively rules out this type of reaction. The dissociation energy of the ion pair was computed to be 25.1 kcal/mol in solution. Given the huge solvation contribution ( $\sim 100$  kcal/mol) to this energy, and a conservative estimate of its accuracy as  $\sim 10\%$ , the above binding energy could well be an overestimate. Thus the ionization of **13C** is considered a definite possibility.

In summary, the barriers associated with the methane–ammonia exchange and the subsequent C–H activation and proton elimination steps are comparable, as are the barriers for the  $\sigma$ -bond metathesis and oxidative addition pathways. Thus once methane is in the first coordination shell, the reaction is predicted to be effectively free energy neutral.

**Methane Activation by *trans*-Platin.** The PES obtained for the methane activation by *trans*-platin is shown in Figure 6. In comparison with *cis*-platin, the initial methane–ammonia exchange is a considerably more energetic process, with the *trans*-platin transition state 2T-TS corresponding to a free energy barrier of  $\sim 44$  kcal/mol, viz.  $\sim 10$  kcal/mol more than for *cis*-platin. In analogy with *cis*-platin, the product of this first reaction is  $[\text{PtCl}_2(\text{CH}_4)(\text{NH}_3)] \cdots \text{NH}_3$  (**5T**), which is  $\sim 8$  kcal/mol less stable than the *cis* isomer **5C**, relative to the respective parent species  $[\text{PtCl}_2(\text{NH}_3)_2]\text{CH}_4$  (**1T** or **1C**). The structures corresponding to this first step are shown in Figure 7.

The  $\sigma$ -bond metathesis pathway (see structures in Figure 8)



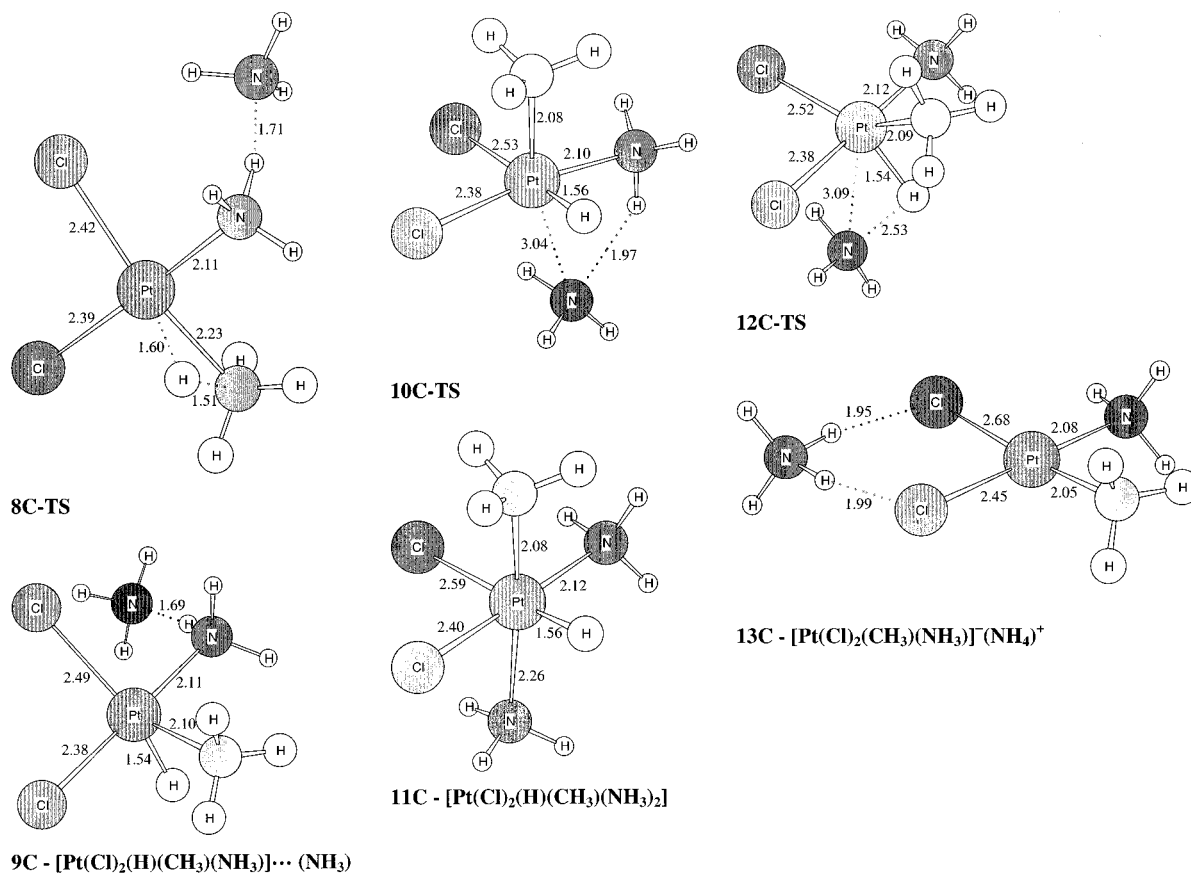


**Figure 5.** C–H activation by oxidative addition in *cis*-platin: Structures of intermediates and transition states.

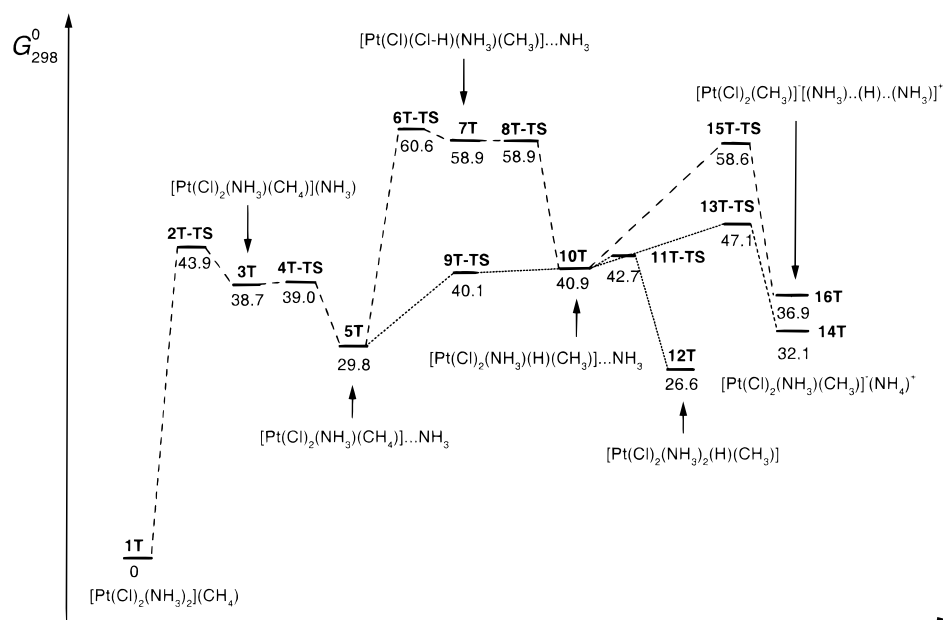


**Figure 6.** Schematic potential energy surface for methane activation by *trans*-platin.

for the activation of a C–H bond of methane appears to be much less favorable than in the case of *cis*-platin. As a proton migrates to one of the chloride ligands, a barrier with a free energy of  $\sim 31$  kcal/mol (relative to **5T**) is encountered, corresponding to a 4-center transition state (**6T-TS**). The free energy of the resulting intermediate, viz. [Pt(HCl)Cl(CH<sub>3</sub>)(NH<sub>3</sub>)]<sup>-</sup>...NH<sub>3</sub> (**7T**), is only marginally lower than that of the transition state **6T-TS**. In contrast with these results, the analogous transition state and product for hydrogen migration in the *trans*-[PtCl<sub>2</sub>(H<sub>2</sub>O)<sub>2</sub>] system were found to be just 16.5

and 6.5 kcal/mol, respectively, above the energy of *trans*-[PtCl<sub>2</sub>(H<sub>2</sub>O)(CH<sub>4</sub>)](H<sub>2</sub>O) in the study of Siegbahn and Crabtree.<sup>17</sup> Furthermore, they believe that the next step, where the proton is transferred from the chloride to the water ligand, is a facile process that results in the formation of [PtCl<sub>2</sub>(CH<sub>3</sub>)]<sup>-</sup>(H<sub>3</sub>O<sub>2</sub>)<sup>+</sup>, where the H<sub>3</sub>O<sub>2</sub><sup>+</sup> moiety is hydrogen bonded to the chlorides. We were unable to find a transition state that would lead to the analogous system, viz. [PtCl<sub>2</sub>(CH<sub>3</sub>)]<sup>-</sup>(N<sub>2</sub>H<sub>7</sub>)<sup>+</sup>. The optimizations consistently yielded a transition state (**8T-TS**) that leads to a 5-coordinate square pyramidal Pt(IV) hydride, [PtCl<sub>2</sub>H(CH<sub>3</sub>)-



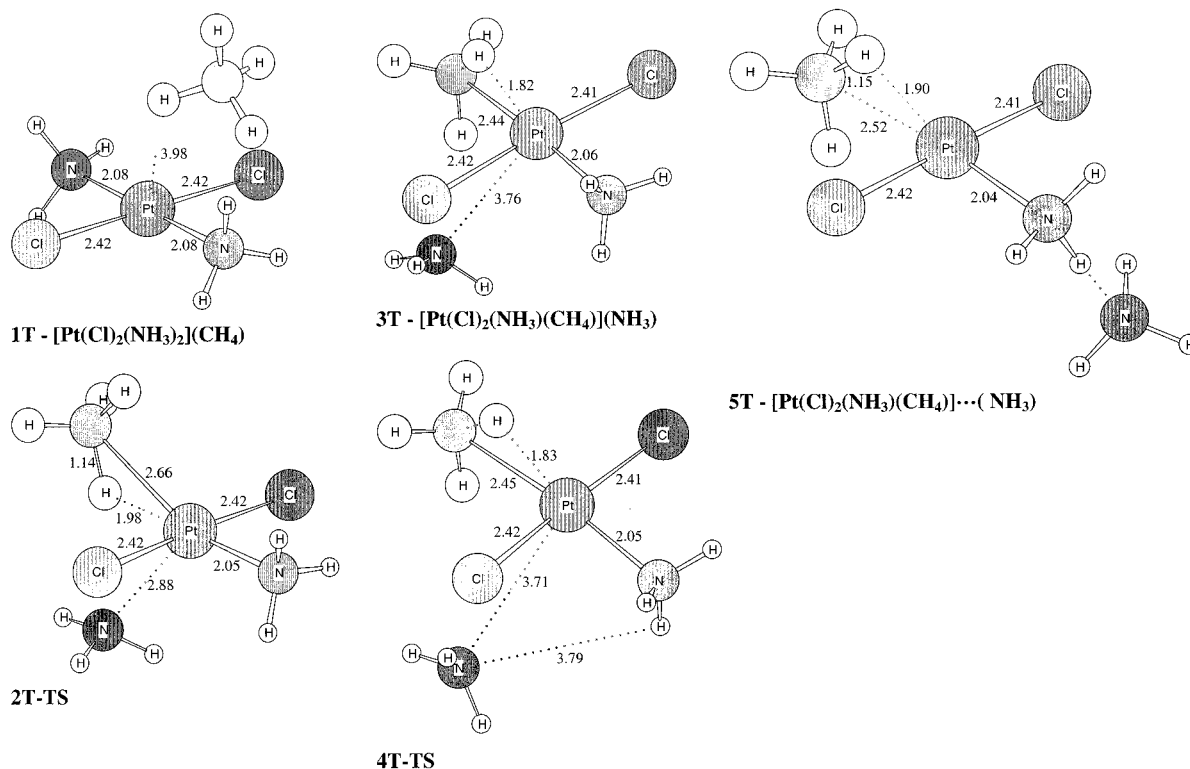


Figure 7.  $\text{CH}_4/\text{NH}_3$  exchange in *trans*-platin: Structures of intermediates and transition states.

$(\text{NH}_3)]\cdots\text{NH}_3$  (**10T**), which is only  $\sim 11$  kcal/mol higher in energy than  $[\text{PtCl}_2(\text{CH}_4)(\text{NH}_3)]\cdots\text{NH}_3$  (**5T**). Interestingly, the analogous intermediate to **10T** in the *cis*-platin activation pathway, viz. **9C**, has a trigonal bipyramidal structure. Although **7T**, with a Pt–ClH bond, may appear somewhat unusual, we note that an iridium complex with an Ir–FH bond has been experimentally observed by Patel and Crabtree.<sup>42</sup>

On exploring the oxidative addition mechanism (see structures in Figure 9), we found that there is a low-energy barrier (**9T-TS**) that directly leads to  $[\text{PtCl}_2\text{H}(\text{CH}_3)(\text{NH}_3)]\cdots\text{NH}_3$  (**10T**). The intermediate **10T** can be further stabilized by allowing it to become hexacoordinate, e.g. by moving the ammonia in the second coordination shell into the appropriate axial position. The resulting *trans*- $[\text{PtCl}_2\text{H}(\text{CH}_3)(\text{NH}_3)_2]$  molecule (**12T**) is in fact the most stable system on the PES. Thus, for *trans*-platin both the  $\sigma$ -bond metathesis and oxidative addition mechanisms will ultimately yield an oxidized Pt(IV) intermediate.

The reduction of **12T** to  $[\text{PtCl}_2(\text{NH}_3)(\text{CH}_3)]^-(\text{NH}_4)^+$  (**14T**) (see structures in Figure 10) is an endothermic process that can take place by returning to the 5-coordinate intermediate **10T**, followed by proton migration via the transition state **13T-TS**. Alternatively, **10T** can rearrange to yield the complex **16T** that can be regarded as a  $[\text{PtCl}_2(\text{CH}_3)]^-(\text{N}_2\text{H}_7)^+$  ion pair, although this is a considerably more energetic process. **16T** is analogous to the product  $[\text{PtCl}_2(\text{CH}_3)]^-(\text{H}_5\text{O}_2)^+$  identified by Siegbahn and Crabtree in their work on the *trans* diaqua complex.<sup>17</sup>

In summary, as in the *cis*-platin system, the methane–ammonia exchange and C–H activation and proton-transfer steps have comparable barriers. In an absolute sense however the barriers are  $\sim 12$  kcal/mol higher than for *cis*-platin. Moreover, in the *trans*-platin system the C–H activation process is predicted to take place predominantly by oxidative addition, with the  $\sigma$ -bond metathesis being no longer competitive with the oxidative mechanism.

The catalysis of methane activation by platins is therefore qualitatively different from that which Siegbahn and Crabtree<sup>17</sup>

found for the Shilov reaction where the catalyst is  $[\text{PtCl}_2(\text{H}_2\text{O})_2]$  and where the reactions of the *cis* and *trans* isomers have comparable energetics, with C–H activation, either by  $\sigma$ -bond metathesis or oxidative addition, being the most energetic steps.

**Charge Distribution and Bonding.** In an effort to better understand the chemistry of C–H activation in terms of simple bonding ideas, we carried out Roby–Davidson and Mulliken population analyses for the parent compounds, *cis*- and *trans*-platin, as well as selected intermediates and products that contribute to the reaction pathways. The results are summarized in Table 4. Although the two methods yield qualitatively similar results, especially with respect to the trends, there are obvious major differences. The Roby–Davidson method assigns a positive charge of  $\sim 0.9$ – $1.3$  e to Pt, while the corresponding Mulliken charges range from  $\sim -0.30$  to  $-0.10$ . Given that formally, at least, platinum in these molecules has an oxidation state of II or IV, an overall negative charge is most likely an artifact. Therefore, as in our previous work on osmium complexes,<sup>48</sup> we prefer to use the Roby–Davidson method to aid our understanding of bonding patterns in terms of simple, chemical concepts. Methane, as ligand, appears essentially neutral, while methyl is negative, with a charge that varies between  $-0.13$  and  $-0.37$  e. Interestingly, methyl is most negative in the least stable *trans* systems **7T** and **10T**. The ammonia moieties appear effectively neutral, but the charge on the chlorines is mostly  $\sim -0.60$  e, except where they are bonded to the hydrogen, as in **7C** and **7T**. As one may expect, the chlorides represent the largest source of charge donation to Pt. The shared electron numbers between two atoms are interpreted as an indication of the covalency of the bond between the atoms. The largest degree of electron sharing occurs between Pt and C in the methyl complexes and between Pt and H in the hydrides, and therefore, only those results are quoted in Table 4. On the basis of this and the computed charges on the methyl and

(48) Craw, J. S.; Bacskay, G. B.; Hush, N. S. *J. Am. Chem. Soc.* **1994**, *116*, 5937.

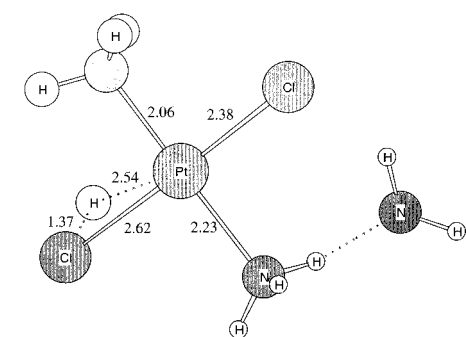
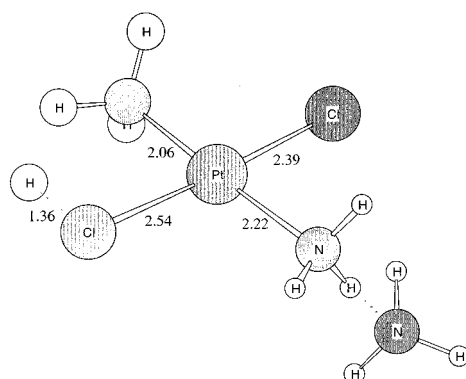
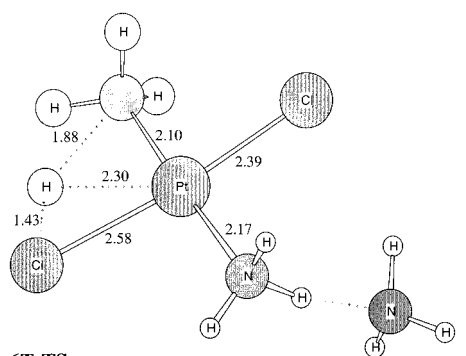


**Figure 8.** C–H activation by  $\sigma$ -bond metathesis in *trans*-platin: Structures of intermediates and transition states.

hydride ligands, we may conclude that the Pt–CH<sub>3</sub> and Pt–H bonds are largely covalent. By contrast, there is considerably less electron sharing between the Pt and the chloride or ammonia ligands. Thus, there appear to be two distinct types of bonding mechanisms: covalent bonding, as characterized by the Pt–CH<sub>3</sub> and Pt–H bonds, and largely electrostatic crystal field type interactions with little covalent character, as in the case of the “classical” ligands NH<sub>3</sub> and Cl<sup>−</sup>. The pattern in the shared electron numbers is roughly reflected in the Mulliken overlap charges. In summary, while describing the methyl hydrido complexes in terms of Pt<sup>4+</sup> and CH<sub>3</sub><sup>−</sup> and H<sup>−</sup> ligands is formally correct, the chemically more accurate description would be in terms of covalent bonds between Pt<sup>2+</sup> and CH<sub>3</sub> and H radicals.

On the basis of the above analysis, the Pt(IV) methyl hydrido complexes could be described in terms of a covalently bonded (H–Pt–CH<sub>3</sub>)<sup>2+</sup> molecule which is able to coordinate up to four ligands, such as chloride and ammonia. As in analogous Pd complexes,<sup>46</sup> such covalent bonding would utilize sd type hybrids of Pt<sup>2+</sup>, which would result in near 90° bond angles. Recalling that the hydride and methyl anions as ligands are known to have strongly trans-influencing and trans-influenced

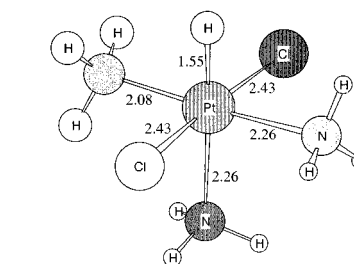
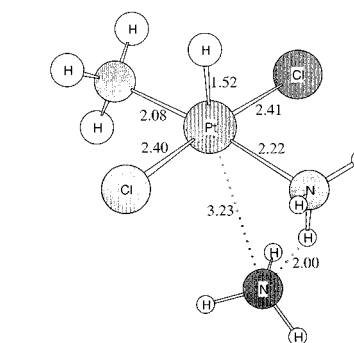
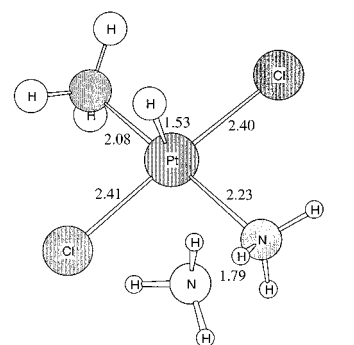
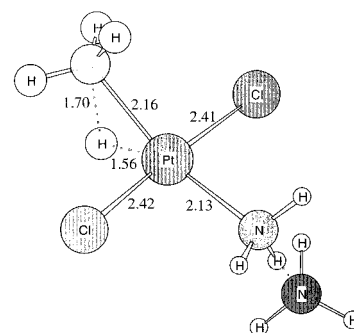


**Figure 9.** C–H activation by oxidative addition in *trans*-platin: Structures of intermediates and transition states.

properties, i.e., a strong preference for not being trans to each other, such behavior may well be a consequence of the covalent bonding between Pt<sup>2+</sup> and the H and CH<sub>3</sub> radicals.

**Relative Stabilities of Isomers of Pt(IV) Methyl Hydrido Complexes.** The structures of the Pt(IV) methyl hydrido complexes identified as intermediates in this work (**9C**, **11C**, **10T**, and **12T**) are such that the methyl and hydride ligands are cis to each other, inasmuch as one is equatorial while the other is axial. However, in our previous work, when exploring the reaction energies associated with oxidative addition mechanisms, where methane adds on to Pt(NH<sub>3</sub>)<sub>2</sub>(OSO<sub>3</sub>H)<sub>2</sub>, Pt(NH<sub>3</sub>)<sub>2</sub>-(OSO<sub>3</sub>H)(H<sub>2</sub>SO<sub>4</sub>), or indeed Pt(NH<sub>3</sub>)<sub>2</sub>(Cl)<sub>2</sub>, the methyl and

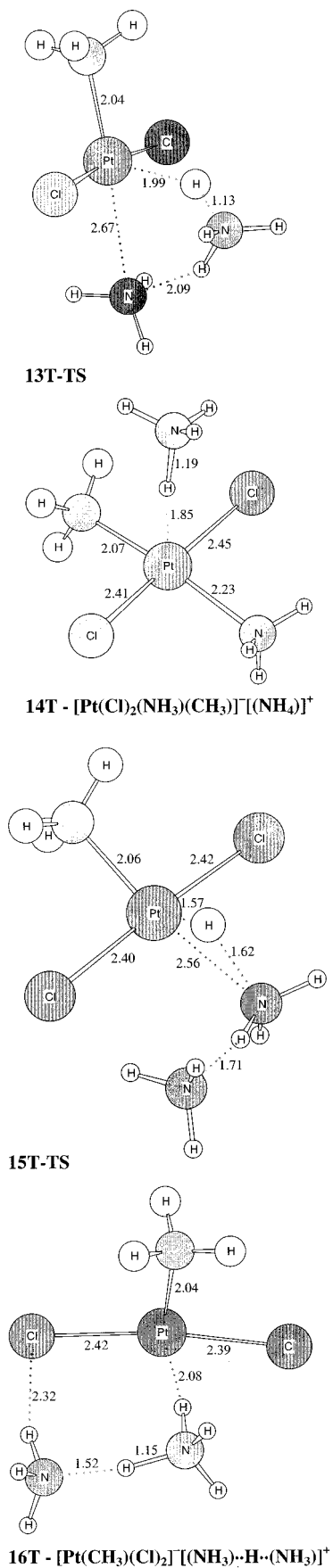


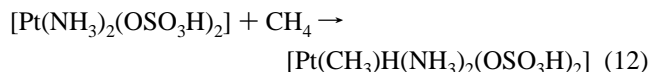
**Figure 10.** Reduction of *trans*-[PtCl<sub>2</sub>H(CH<sub>3</sub>)(NH<sub>3</sub>)<sub>2</sub>]: Structures of intermediates and transition states.

hydride ligands were placed *trans* to each other as axial ligands. As pointed out by Labinger,<sup>49</sup> and also discussed above, given

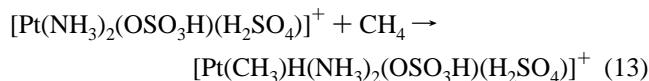
the strongly *trans*-directing natures of these two ligands, the resulting *trans* Pt(IV) complexes would be expected to be significantly less stable than the *cis* isomers.

To quantify the importance of such *trans* influence in the context of methane activation, a detailed comparison of the relative stabilities of such *cis* and *trans* isomers has also been carried out, for both the current systems, as well as those studied in our previous work. The results are summarized in Table 5. The energies of the four isomers where CH<sub>3</sub> and H are *cis* to each other are within ~7 kcal/mol of each other, but they are ~32–40 kcal/mol lower than the energy of the fifth isomer where CH<sub>3</sub> and H are *trans* to each other, as expected on the basis of *trans* influence. The variations in energy among the bisulfate complexes are similar to that for the simple chlorides, except where the bisulfates are *trans* to each other, with CH<sub>3</sub> and H *cis*. The higher energy of this particular isomer can be attributed to the absence hydrogen bonding between bisulfates in this *trans* complex. The relative stabilization that results from hydrogen bonding in molecules where the bisulfates are *cis* to each other was estimated by comparing the energies of the bisulfate dimer moieties at the geometries they assume in the first two isomers from Table 5. The energy of the *trans* configuration was computed to be 22.9 kcal/mol higher than for the *cis*. This is in near-perfect agreement with the energy difference of 20.1 kcal/mol that had been obtained for the corresponding Pt complexes.

In light of this study we conclude that contrary to our earlier findings, the oxidative addition type reactions



and



could be thermodynamically viable. Using the lowest energy structures from Table 5 for the above methyl hydrido complexes (with the ammonias *trans* to each other), the reaction enthalpies in solution at 298 K for reactions 12 and 13 were computed to be 5.2 and 10.4 kcal mol<sup>-1</sup>, respectively. The corresponding reaction free energies are 17.1 and 20.6 kcal mol<sup>-1</sup>, while at 473 K and a pressure of 500 psi the free energies are 20.7 and 23.2 kcal mol<sup>-1</sup>.

## Conclusion

In our study of C–H activation of methane catalyzed by *cis*- and *trans*-platin in aqueous solution, where the initial step is the replacement of an ammonia ligand by methane, we found that once that substitution has taken place, the barriers to the subsequent activation and proton elimination steps are comparable with those of the initial substitution reaction. However, in contrast with the Shilov reaction studied by Siegbahn and Crabtree,<sup>17</sup> the initial energy barriers are substantially higher in the case of the platins, as are the overall heats and free energy changes of the overall substitution reactions. This can be traced to the relatively strong platinum–ammonia bond. In the case of *cis*-platin the C–H activation is expected to occur by both  $\sigma$ -bond metathesis and oxidative addition. The energy barriers associated with these two distinct pathways were found to be comparable. However, in the *trans*-platin system the C–H activation process is predicted to take place predominantly by

(49) Labinger, J. A. Private communication.

**Table 4.** Results of Roby–Davidson (RD) and Mulliken Population Analyses on Selected Reactants, Intermediates, and Products: RD and Mulliken Charges on Pt and Ligands and RD Shared Electron Numbers and Mulliken Overlap Populations (Mulliken Results in Parentheses)

|                      | RD and (Mulliken) charges on Pt and ligands |                                    |   |                              |      | RD shared electron nos.<br>(Mulliken overlap populations) |               |
|----------------------|---|------------------------------------|---|------------------------------|------|---|---------------|
|                      | Pt  | CH <sub>3</sub> or CH <sub>4</sub> | NH <sub>3</sub> or NH <sub>4</sub> <sup>+</sup> | Cl                           | H    | Pt/C  | Pt/H          |
| <i>cis</i> -platin   | 0.96 (0.05)                                 |                                    | 0.11 (0.40)                                     |                              |      |   |               |
| <b>5C</b>            | 0.95 (−0.24)                                | 0.05 (0.40)                        | 0.10 (0.17), 0.03 (0.42)                        | −0.60 (−0.38), −0.53 (−0.37) |      | 0.06 (0.16)   | 0.07          |
| <b>7C</b>            | 0.85 (−0.23)                                | −0.17 (0.15)                       | 0.14 (0.16), 0.05 (0.40)                        | −0.55 (−0.35), −0.41 (−0.12) | 0.03 | 0.54 (0.35)   | 0.01 (−0.05)  |
| <b>9C (IV)</b>       | 1.28 (−0.13)                                | −0.13 (0.30)                       | 0.15 (0.17), 0.01 (0.44)                        | −0.60 (−0.32), −0.72 (−0.47) | 0.00 | 0.43 (0.34)   | 0.65 (0.27)   |
| <b>13C</b>           | 0.85 (−0.15)                                | −0.20 (0.10)                       | 0.63 (0.71), 0.15 (0.42)                        | −0.68 (−0.47), −0.77 (−0.62) |      | 0.52 (0.36)   | 0.00 (−0.01)  |
| <i>trans</i> -platin | 0.98 (−0.09)                                |                                    | 0.11 (0.49)                                     |                              |      |   |               |
| <b>1T</b>            | 0.95 (−0.14)                                | 0.08 (0.04)                        | 0.03 (0.49), 0.14 (0.49)                        | −0.59 (−0.43), −0.62 (−0.45) |      | 0.00 (0.01)   |               |
| <b>5T</b>            | 0.97 (−0.31)                                | 0.08 (0.47)                        | 0.11 (0.17), 0.07 (0.51)                        | −0.64 (−0.43), −0.60 (−0.41) |      | 0.07 (0.20)   | 0.08 (0.08)   |
| <b>7T</b>            | 0.85 (−0.31)                                | −0.37 (0.10)                       | 0.09 (0.14), 0.03 (0.36)                        | −0.65 (−0.44), −0.13 (+0.15) | 0.19 | 0.46 (0.39)   | −0.01 (−0.03) |
| <b>10T (IV)</b>      | 1.29 (−0.11)                                | −0.25 (0.30)                       | 0.09 (0.15), 0.00 (0.37)                        | −0.65 (−0.37), −0.62 (−0.34) | 0.14 | 0.39 (0.36)   | 0.69 (0.25)   |
| <b>14T</b>           | 0.99 (−0.58)                                | −0.37 (0.22)                       | 0.74 (−0.47), 0.10 (0.38)                       | −0.74 (−0.47), −0.71 (−0.43) |      | 0.43 (0.39)   | 0.00 (−0.01)  |

**Table 5.** Relative Gas-Phase Energies (without Zero-Point Vibrational Corrections) of Isomers of [Pt(X)(NH<sub>3</sub>)<sub>2</sub>(H)(CH<sub>3</sub>)] (X = Cl, OSO<sub>3</sub>H) Computed at the B3LYP/epc-DZ Level of Theory (in kcal/mol)

| X                               |     |      |     |     |      |
|---------------------------------|-----|------|-----|-----|------|
| Cl <sup>−</sup>                 | 0.0 | 2.5  | 6.1 | 7.1 | 39.5 |
| OSO <sub>3</sub> H <sup>−</sup> | 0.0 | 20.1 | 4.2 | 5.2 | 42.1 |

oxidative addition, as the  $\sigma$ -bond metathesis was found to be associated with a much higher barrier, in further contrast with the Shilov reaction where the two pathways were found to be comparable with regard to their activation energies. A valuable finding of our study is that, in line with accepted ideas on trans influence, the methyl and hydride ligands in the Pt(IV) complexes that arise in the oxidative addition reactions are always *cis* to each other.

However, the results of the Roby–Davidson analyses suggest that the Pt–H and Pt–CH<sub>3</sub> bonds are best described as covalent bonds. The possible consequence of this is that the strongly trans-influencing and trans-influenced properties of the hydride

and methyl anions, and hence their preference to be *cis* to each other, may be associated with the tendency of the parent radicals to form covalent bonds with Pt<sup>2+</sup>.

In light of the above findings the energies of several Pt(IV) methyl hydrido bisulfate complexes were also recalculated. The new results provide evidence for the thermodynamic feasibility of oxidative addition of methane to catalysts such as [Pt(NH<sub>3</sub>)<sub>2</sub>(OSO<sub>3</sub>H)<sub>2</sub>] or [Pt(NH<sub>3</sub>)<sub>2</sub>(OSO<sub>3</sub>H)(H<sub>2</sub>SO<sub>4</sub>)]<sup>+</sup>.

**Acknowledgment.** We are pleased to acknowledge the helpful comments of Professor Henry Taube (Stanford University) and also those of Professor J. A. Labinger (California Institute of Technology) concerning the trans-directing properties of methyl and hydride ligands and their importance in oxidative addition mechanisms.

**Supporting Information Available:** Table S1, containing the total electronic energies (in  $E_h$ ) of all molecular species studied in this work (PDF). This material is available free of charge via the Internet at <http://pubs.acs.org>.

JA993015+